Beyond energy balance in agrivoltaic food production: Emergent crop traits from color selective solar cells

Melodi Charles[1], Brianne Edwards[1], Eshwar Ravishankar[2#a], John Calero[1#b], Reece Henry[3], Jeromy Rech[4], Carole Saravitz[1], Wei You[4], Harald Ade[3], Brendan O'Connor[2], Heike Sederoff[1*]

[1]Department of Plant and Microbial Biology, North Carolina State University, Raleigh, North Carolina, United States of America

[2]Department of Mechanical and Aerospace Engineering and Organic and Carbon Electronics Laboratories, North Carolina State University, Raleigh, North Carolina, United States of America

[3]Department of Physics and Organic and Carbon Electronics Laboratories, North Carolina State University, Raleigh, North Carolina, United States of America

[4]Department of Chemistry, University of North Carolina, Chapel Hill, North Carolina, United States of America

[#a]Current Address: Department of Horticulture, North Carolina State University, Raleigh, North Carolina, United States of America

[#b]Current Address: Pairwise Inc., Durham, North Carolina, United States of America

*Corresponding Author

hwsedero@ncsu.edu (HS)

Abstract

Semi-transparent organic solar cells (ST-OSCs) offer new agrivoltaic opportunities to meet the growing demands for sustainable food production. The tailored absorption/transmission spectrum of ST-OSCs not only impacts the power generated, but also aspects of crop growth, development and responses to the biotic and abiotic environments. The general relationships between these variables are unknown. Here, we grow red oak leaf lettuce (*Lactuca sativa*), a traditional greenhouse crop, under three different ST-OSC filters and observe little overall differences on productivity in response to the altered light exposure. In contrast, several key traits involving nutrient content and nitrogen utilization as well as plant defense against herbivory and pathogens are modified over the controls under select OSCs. Overall, our genomic analysis reveals that lettuce production exhibits beneficial traits under exposure from select ST-OSCs. ST-OSCs integrated into greenhouses are, therefore, not only a promising technology for energy-neutral crop production as previously shown but can deliver benefits beyond those based on energy-balance considerations.

Introduction

Greenhouses enable the production of food crops and ornamental plants year-round outside of their natural environment and growth zones. Due to the enclosed nature of greenhouses, water and fertilizer use can be well controlled and recycled. Furthermore, greenhouses do not require the use of herbicides and need only low quantities of pesticide. A comparative analysis of tomato production showed that greenhouse productivity in New York was 12-fold higher than that of Florida fields (De Villiers, et al., 2009). However, this seemingly ideal system for plant productivity requires large amounts of energy for climate control and supplemental lighting, which reduces its economic and environmental sustainability. Field-grown tomatoes in Florida consumed 7.1 MJ energy/kg tomatoes, while greenhouse production in upstate New York required 53 MJ/kg (Barbosa et al, 2015).

While other solar-powered greenhouses do improve the sustainability of food production, they require either additional land in the form of solar farms or a reduction in yield in the case of opaque rooftop solar cells (Hassanien et al, 2016). Fully enclosed (sole-source) container farms are an alternative to greenhouse cultivation with a lower cost for climate control, but they suffer from high energy costs for artificial lighting that prevent their economic viability for crops other than microgreens or lettuce (Pattison, et al., 2018a). To utilize natural sunlight for both crop growth and electricity, wavelength-selective semi-transparent organic solar cells (ST-OSCs) can be integrated into the structure of the greenhouse itself. By adding solar panels to the greenhouse roof, the cost of crop production can be kept close to the cost of conventional and photovoltaic-adjacent greenhouse systems in favorable climates without requiring additional land (Hollingsworth, et al., 2020a). ST-OSC systems have the added benefit of allowing more light to reach the plants to avoid the yield losses seen with opaque systems. OSC greenhouses reduce global warming potential by 36% with only a 6% decrease in net production cost, compared to conventional greenhouses (Hollingsworth, et al., 2020b), while avoiding the light limitations of container agriculture. However, using ST-OSCs systems in greenhouses affects both the light quantity and the light spectrum (i.e. quality) available to the plants. By choosing different combinations of organic semiconductors serving as electron donor and acceptor pairs for the

active layer, the absorption spectrum of the OSCs can be modulated, and with that, the spectrum available to the plants can be further controlled (Xiao, et al., 2017) (Fig. 1). The wide variety of OSC active layers allows growers to account for the specific light requirements of the crop as well as the energy requirements of the climate and season. These net zero energy greenhouses have been shown to be feasible by taking advantage of this flexibility (Ravishankar, et al., 2020; Ravishankar, et al., 2022).

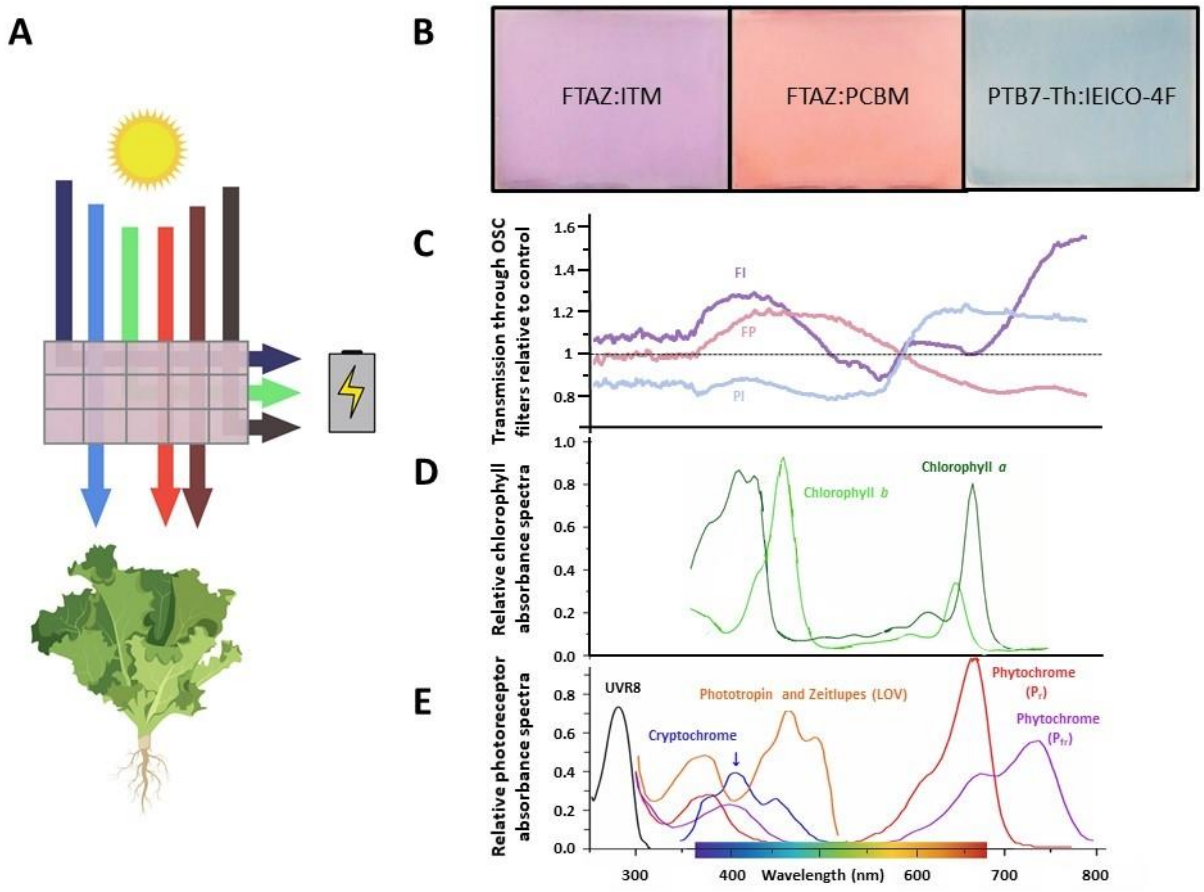

Figure 1. Wavelength selectivity of OSC devices
a) Schematic of a wavelength-selective OSC device. Specific wavelengths of light are harvested to generate electrical energy to power the greenhouse. The wavelengths most important for photosynthesis (blue, red and far-red) are selectively transmitted through the device to grow greenhouse crops. b) The OSC filters are named for the two organic molecules that determine their color and transmission spectrum. Different donor and acceptor molecules can be chosen to tune the wavelengths that reach the plants below. c) Ratio of light transmission through the OSC filters relative to the light transmitted through the control. Each filter varies in relation to the control and to each other over PAR and in the far-red region (700-750 nm). d) Absorption spectra of plant chlorophylls. Chlorophyll a and b harvest light energy from sunlight to power photosynthesis over PAR (400-700 nm), especially in the blue and red regions (adapted from Eichhorn Bilodeau, et al., 2019). e) Absorption spectra of photoreceptors. UVR8 absorbs UV light. Cryptochromes, phototropins and zeitlupes absorb primarily blue light. Phytochromes absorb red and far-red light (adapted from Eichhorn Bilodeau, et al., 2019)

Plants depend on light for their energy supplied by photosynthesis. Light harvesting antenna complexes contain large numbers of chlorophylls with absorption maxima in the blue (400-500 nm) and red light (600-700 nm) regions of the visible spectrum (Eichhorn Bilodeau, et

al., 2019) (Fig. 1d). Other chromophores, such as carotenoids or anthocyanins, are produced to absorb and divert excess photons to protect the photosynthetic machinery (Tanaka, et al., 2008). Based on the absorption spectra of the chlorophylls, the most important wavelengths for photosynthesis are 400-700 nm and are collectively referred to as photosynthetically active radiation (PAR). PAR is measured as photosynthetic photon flux density (PPFD) and is used to measure the amount of light available for plants. A broader measurement, the total photon flux density (TPFD), accounts for the full range of wavelengths sensed by plants (Zhen and Bugbee, 2020; Kohler and Lopez, 2021; Kim, H., et al., 2019).

Because light is the only energy source for plants, their entire growth and development is dependent upon and regulated by changes in their light environment. Plants have evolved a complex network of additional chromophores called photoreceptors that sense light quality, intensity, direction and even polarity in the 400-700 nm range of PAR and beyond (Galvao and Fankhauser, 2015) (Fig. 1e). These photoreceptors are not involved in energy harvesting but provide information about light conditions to adjust the plant's growth and development in a process called photomorphogenesis (Galvao and Fankhauser, 2015). Photoreceptors sense the dynamic changes in the natural light environment that occur on a second to minute scale (e.g. cloud cover), daily scale (e.g. time of day) and seasonal scale (e.g. day length) (Naganoe et al. 2019). This information is used to regulate growth and development through large integrated gene networks with other environmental factors such as nutrient availability and temperature (Abbas, et al., 2014; Chen, et al., 2016; Hahm, et al., 2020). These gene networks influence many factors important for crop production, including height, nutrient content and the timing of flowering and fruit production (Susan A. Dudley, et al., 1999; Guo, et al., 1998; Park, et al., 2007).

The light environment created by OSCs is complex, with each organic semiconductor donor and acceptor combination creating a unique transmission spectrum that varies across the wavelengths important for photosynthesis and photomorphogenesis. This complexity makes it difficult to predict plant growth in OSC-powered greenhouses. One OSC crop production model considered only photosynthesis to calculate a crop growth factor based on the relative photosynthetic efficiency of each photon across PAR and predicted the effect of OSC transmission spectra on crop yield (Emmott, et al., 2015). A more complex model considered the red/blue (R/B) ratio of the OSC transmission spectrum as well as light intensity to begin to address the effect of altered spectra on photomorphogenesis (Ravishankar, et al., 2022). Growth and yield studies using peppers (Zisis, et al., 2019) and tomatoes (Waller, et al., 2021) have been promising in greenhouses partially covered with OSCs panels (~22% and ~50%, respectively). However, these systems are limited in their energy production potential due to the large surface area that was reserved to allow unfiltered sunlight to reach the plants. We have previously shown that overall growth of lettuce (*Lactuca sativa* L. var. "red oak leaf") is not significantly impacted when grown exclusively under OSC-filtered light with different spectra (Ravishankar, et al., 2021). This makes a strong case for growing lettuce, the second largest fresh vegetable grown in the US by acreage and value (USDA, National Agricultural Statistics Service, 2020), under near complete shading from semi-transparent OSCs. This design maximizes surface area dedicated to solar panels, resulting in more energy production. However, in our previous study as well as in those mentioned earlier, it is difficult to distinguish between the effects of the overall reduction in light and any spectral effects.

To expand our understanding of how plants respond to both the quantity and quality of OSC-filtered light, an in-depth analysis of gene expression is needed. There are roughly 40,000

genes in the lettuce genome (Reyes-Chin-Wo, et al., 2017), and many of these are upregulated (increased in expression) or downregulated (decreased in expression) in response to environmental cues. These genes are organized into interrelated networks that result in specific phenotypic changes, such as the initiation of flowering (Khan, et al., 2014). The transcriptome is the qualitative and quantitative presence of all expressed genes, and therefore reflects the use and regulation of an organism's genes at a given time. Comparative transcriptome analysis from plants grown under different light environments can be used as a detection tool to characterize the environmental impact of environment on the gene networks involved in photosynthesis and photomorphogenesis.

We present here experiments that enabled us to distinguish the qualitative and quantitative effects of OSC filters on gene expression, nutrient content and nitrogen utilization in lettuce. Plants were grown under one of three previously studied OSC filters that were selected based on their spectral complementarity with chlorophyll and photoreceptor absorbance and ease of fabrication: FTAZ:IT-M (FI), FTAZ:PCBM (FP) and PTB7-Th:IEICO-4F (PI) (Ravishankar, et al., 2021) (Fig. 1). Plants grown under OSC filters were similar in size to those grown under a spectrally neutral shaded control. Furthermore, we demonstrate modifications in gene expression detected through a transcriptome analysis that point to important changes in crop physiology, including flowering, nutritional content and fertilizer utilization in response to the altered light spectra.

Materials and Methods

Filter fabrication

OSC filters were made as previously described (Ravishankar, et al., 2021). Solutions of the organic semiconductor active layers were wire bar-coated onto glass substrates. A second sheet of glass was adhered under heat to each of the glass substrates with ethylene vinyl acetate films for encapsulation. Optical epoxy (Norland 63) was cured around the edge of the filter stack as an additional seal. Twelve of these filters, each 20x10cm, were arranged in a single layer above a layer of PEDOT:PSS (PH1000, Hareus) coated onto a PET substrate to simulate the transmission of full OSC devices for each filter treatment.

Plant growth and lighting conditions

Red oak leaf lettuce (*Lactuca sativa*) was grown as previously described with the addition of a PPFD controlled (PC) experiment (Ravishankar, et al., 2021). The PC experiment was a comparison of the influence of the light spectra on plant physiology, whereas the HC experiment was a more real-life scenario where all filters are at the same height to model the roof of a greenhouse and therefore produce different TPFD due to the differences in filter transmission. All light that reached the plants was filtered through either OSC filters or one of two control conditions: clear glass or glass shaded with mesh that absorbed light evenly across the visible and far-red spectrum. Plants were grown inside growth boxes covered with these filters to test nearly 100% OSC roof coverage. The light intensity of the PC experiment control treatment was further reduced with the addition of a spectrally neutral shade to bring the control's PPFD closer to that of the filter treatments. TPFD was also measured for each treatment from 400 - 750 nm. The UV region of photoreceptor absorbance was excluded from TPFD because UV radiation

within the growth chamber was negligible. Treatments are referred to by both their filter and their designation in either the PC or HC experiments. For example, FI_PC is the FTAZ:IT-M filter treatment in the PPFD controlled experiment.

32 seedlings were sown on soil and germinated in a growth chamber with metal halide and incandescent lighting to approximate natural sunlight. Two seedlings per pot, eight pots per treatment were used in each replicate and grown inside plexiglass growth boxes with either an OSC filter, a clear glass or a shaded control on top to simulate a greenhouse roof. All other sides of the boxes were covered with reflective mylar to prevent plants from receiving ambient white light. To avoid positional effects on growth, pots were rotated every two days in the dark to prevent white light exposure. Plants were watered and fertilized via an automatic irrigation system. Eight plants from each treatment were harvested at 21 days post germination (transplant stage) and the remaining eight plants from each treatment at 35 days post germination (harvest stage). Four plants from each harvest per box were used for biomass measurements, while the remaining four were used for tissue sampling. For the Height Controlled (HC) experiment, growth boxes were arranged at a consistent height to simulate a true greenhouse environment. Boxes were elevated or lowered so that PPFD was consistent for all treatments in the PC experiment using a quantum sensor (LI-190R, LI-COR, Inc., USA). Additional shading that absorbed light equally across the measured spectrum (300-900 nm) was required for the PC experiment control box. Reported PPFD and TPFD were measured using a spectrophotometer (Black Comet-SR, Stellar Net, Inc., USA). Five replications of the experiment were conducted of the PPFD controlled (PC) experiment. Three replications were conducted of the height controlled (HC) experiment.

Biomass measurements

Measurements of fresh weight, dry weight, leaf area and leaf number were collected as previously described (Ravishankar, et al., 2021) at Day 21 and Day 35 after germination. The 21-day early harvest corresponds to the age when young lettuce is typically transplanted. Both fresh and dry weights are above ground measurements that do not include root tissue. Dry weight was measured after leaves were dried at 65°C for three days. Leaf area was measured by leaf meter (LI-3000, LI-COR, Inc., USA) and summed per plant. Leaf number was also summed by plant and excluded any emerging leaves less than 1 cm in length.

Extraction and quantification of secondary metabolites

Secondary metabolites were extracted from ground frozen leaf tissue as previously described (Ravishankar, et al., 2021; Sims and Gamon, 2002). Leaf tissue was collected from four harvest stage plants and immediately frozen in liquid nitrogen and stored until ground. Ground frozen leaf tissue was weighed and suspended in extraction buffer. A BioTek Synergy HT microplate reader (BioTek Instruments, USA) was used to measure absorbance.

Photosynthetic data collection

A LI-6400XT (LI-COR, Inc., USA) was used to collect photosynthetic data as previously described (Ravishankar, et al., 2021). Two sample measurements were collected per leaf, two leaves per plant and four plants per treatment beginning five days before the final harvest.

Photosynthesis was measured *in situ* inside the growth boxes to observe the impact of the light intensity and spectrum created by the OSC filters. The chamber door was kept closed during data collection to minimize changes to the environment and a black cloth was used to block ambient white light from entering around the equipment. A CO_2 scrubber was used to prevent elevated CO_2 levels from researcher exhalation. PPFD was monitored as measured by the instrument to ensure lighting conditions remained consistent throughout the data collection for each treatment.

Statistical analysis of physiological data

Physiological data was analyzed by ANOVA and Tukey post-hoc test where $p<0.05$. Treatments that share a letter were not significantly different. Physiological data reported in the body of this report were collected from the same replication of the experiments used in the transcriptome analysis. Photosynthetic data were further analyzed by dividing by the PPFD recorded at time of measurement to identify potential effects of small changes in light intensity in the PC experiment. To minimize variation between replications, the biomass and secondary data was normalized relative to the control treatment within each round. PC experiment biomass and secondary metabolite data were collected from five total replications of the PC experiment and normalized by replicate relative to their respective controls. Two replicates were performed simultaneously in the same growth chamber and were normalized together. HC experiment physiological data were collected from three replications previously reported and normalized as described above (Ravishankar, et al., 2021). These normalized data are presented in the supplementary information.

RNA extraction

Mature leaf tissue was collected from four plants per treatment in one replicate and ground in liquid nitrogen. The PureLink RNA Mini on-column kit with TRIzol (ThermoFisher Scientific, Inc., USA) was used to extract total RNA. An on-column DNAse treatment with additional off-column DNAse I treatments were used to remove DNA contamination. The mRNA library preparation and sequencing were performed by BGI Genomics Co., Ltd. (Shenzhen, China) with polyA selection by an oligo dT library. All 32 samples were multiplexed, pooled and loaded together. Sequencing was conducted on a DNBSEQ^{TM} Technology Platform.

Transcriptome analysis

Raw reads were checked for quality standards using FastQC (v. 0.11.9) (http://www.bioinformatics.babraham.ac.uk/projects/fastqc/) and only high-quality read pairs (base score above Q30) were subject to downstream processing. Read pairs were aligned to the *L. sativa* cv. Salinas RefSeq genome assembly version 7 (genome ID: 5962908) using HISAT2 (v. 2.2.1) with default parameter settings (Kim et al., 2015). Genes with multiple copies undifferentiated in the genome annotation were assigned numbers in the order they are referred to in the text (e.g. *HY5-1*). Mapped reads were assigned to genomic features based on Lsat_Salinas_v7 annotations using featureCounts (v. 2.0.1) (Liao, et al., 2014). Read counts were summarized at the gene level and zero-count genes were removed prior to further analysis. Raw data and counts have been deposited in NCBI's Gene Expression Omnibus (Edgar, et al., 2002)

and are accessible through GEO Series accession number GSE180179 (https://www.ncbi.nlm.nih.gov/geo/query/acc.cgi?acc=GSE180179).

Differential expression analysis was performed in R using the edgeR package (v. 3.34.0) (Robinson, et al., 2010; McCarthy, et al., 2012). The estimateGLMCommonDisp function was used to estimate a common gene-wise dispersion parameter suitable for all genes and evaluated on an individual basis and likelihood ratio tests were performed to test for differential expression of genes within pairwise treatment groups. For each test, a single treatment (OSC filter) group was compared to the control (clear or shaded glass) treatment and significance was evaluated based on the Benjamini Hochberg adjusted p-value (threshold of FDR<0.05). A second round of analysis was performed by comparing each treatment in the HC experiment with the corresponding treatment in the PC experiment with the same spectrum (e.g. HC control/PC control).

Network analysis

A transcriptome analysis was conducted to detect gene expression differences caused by the variation in filter spectra in the HC and PC experiments. The transcriptome can provide a snapshot of environmental responses that are not immediately obvious in the plant's phenotype until tested. It is often used to identify emergent traits caused by the combination of changes in the expression of the tens of thousands of genes in the genome. To examine global patterns of gene expression in response to the OSC filters, a network-based approach was used to identify distinct groups of co-expressed genes that shared a similar relationship with the filter-specific light spectra and were common to both the PC and HC experiments. Gene networks were constructed using an unsupervised learning approach on the transcriptome data from the PC and HC datasets independently. The resulting networks were used to build a common consensus network containing clusters of genes (i.e. modules) that are shared between the two networks.

To identify specific genes and gene clusters associated with differences in light quality, weighted gene correlation network analysis was performed on the transcriptome dataset. Normalized read counts were extracted using the edgeR cpm function and log-transformed counts per million were used as input for weighted correlation network analysis (WGCNA) (v. 1.69) (Robinson, et al., 2010; Langfelder and Horvath, 2008; Langfelder and Horvath, 2012). To reduce spurious correlations, genes with consistently low expression (less than two read counts) for four or more samples were removed prior to analysis. With the remaining 24,171 genes, expression similarity was calculated for both the HC and PC datasets using the Pearson correlation metric, and a signed adjacency matrix was constructed for both datasets using a soft-threshold power of 7 to satisfy the scale-free network topology criterion. The network adjacency matrix was then used to calculate the topological overlap for each of the datasets separately. Average linkage hierarchical clustering was performed on the topological overlap dissimilarity matrices, and modules were detected using the dynamic tree cutting algorithm. To compare the HC and PC networks, topological overlap measures were used to scale the HC and PC networks prior to consensus module detection.

Results

Light conditions under OSCs

Boxes topped with OSC filters were designed to house the lettuce within a climate-controlled growth chamber equipped with lights that approximated the spectrum of natural sunlight (Ravishankar, et al., 2021) (Fig. S13). In our previous study, the distance from the light source to the top of each growth box was kept constant to simulate the irradiation on the roof of actual greenhouses (Ravishankar, et al., 2021). This design is referred to here as the height controlled (HC) experiment because the growth boxes were positioned at the same height from the floor of the growth chamber. Due to the unique transmission spectra of the OSC filters, the overall light intensity as well as the spectra varied between treatments in the HC experiment. To differentiate between light intensity and spectral effects on plant growth, we added an additional PPFD controlled (PC) experiment by adjusting the distance from the light source and height of the growth boxes to attain comparable amounts of illumination from 400-700 nm on the plants in all four treatments (Fig. 2, Table 1).

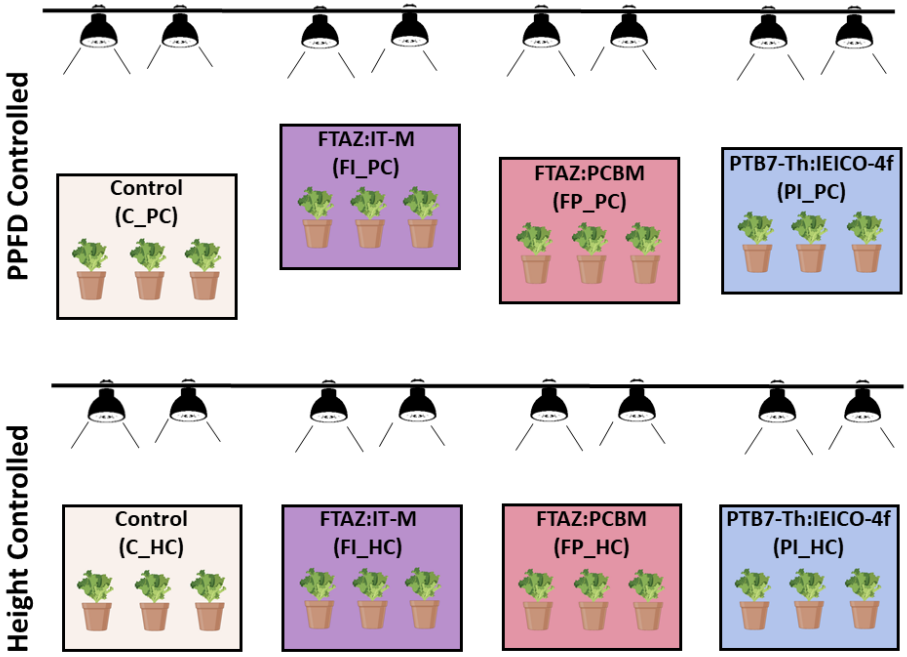

Figure 2. Experimental design of PPFD Controlled (PC) and Height Controlled (HC) experiments
Schematic of the experimental design. The heights of the PC experiment boxes were adjusted so that similar amounts of light reached the plants in each treatment. The HC experiment treatments were arranged at the same height and distance from the chamber light source so that the filters on top of the boxes received the same amount of light to model real-world greenhouse conditions. Created with BioRender.com.

Treatment	C_PC	FI_PC	FP_PC	PI_PC	C_HC	FI_HC	FP_HC	PI_HC
Blue (400-500nm) (% of TFPD)	36 (14%)	52 (15%)	31 (12%)	47 (16%)	107 (14%)	60 (14%)	53 (12%)	78 (15%)
Green (500-600nm) (% of TFPD)	76 (30%)	91 (27%)	64 (25%)	95 (32%)	223 (30%)	111 (27%)	119 (26%)	158 (31%)
Red (600-700nm) (% of TFPD)	121 (48%)	169 (49%)	138 (54%)	136 (45%)	353 (47%)	205 (50%)	243 (53%)	236 (46%)
Far-red (700-750nm) (% of TFPD)	20 (8%)	30 (9%)	23 (9%)	21 (7%)	60 (8%)	37 (9%)	41 (9%)	39 (8%)
PPFD (400-700nm)	233	312	233	279	684	376	415	473
TFPD (400-750 nm)	253	342	256	300	743	413	457	511

Table 1. Light intensity and spectra under OSC filters
Breakdown of the photon flux (μmol m^{-2} s^{-1}) reaching the plants by color measured at the end of the experiments. The percentages of each color relative to the total photon flux density (TPFD) were consistent for each filter in both experiments. Large variations were seen in the amount of light (PPFD and TFPD) that reached the plants inside the boxes in the HC experiment.

Lettuce biomass was not significantly altered by OSC filters

The biomass results of the HC experiment were previously published (Ravishankar, et al., 2021). Select data are repeated here to compare to the results of the PC experiment. Although there were no statistically significant biomass differences in the HC experiment at this stage (Fig. S2), the FI_HC treatment had significantly higher leaf area and number, relative to the control, by the final 35-day harvest stage in the replicate used in the transcriptome analysis (Fig. 3e, f; S1). When the HC experiment was replicated and the results were normalized relative to the control treatment of each replicate, the differences in leaf area and number were no longer significant but a small yet statistically significant difference was seen in dry weight between the PI_HC treatment and control (Fig. S6). Surprisingly, plants in the FI_HC treatment received ~300 μmol m^{-2} s^{-1} less light than the control and had fresh weights, dry weights and leaf numbers closest to the control.

As expected, there were fewer differences between treatments when light intensity was controlled. There were no significant differences in biomass for plants receiving the same amount of light in the PC experiment at the transplant (Fig. S2) or harvest stage (Fig. 3a, b). The spectral differences between the three OSC filters alone were not great enough to have a significant effect on biomass.

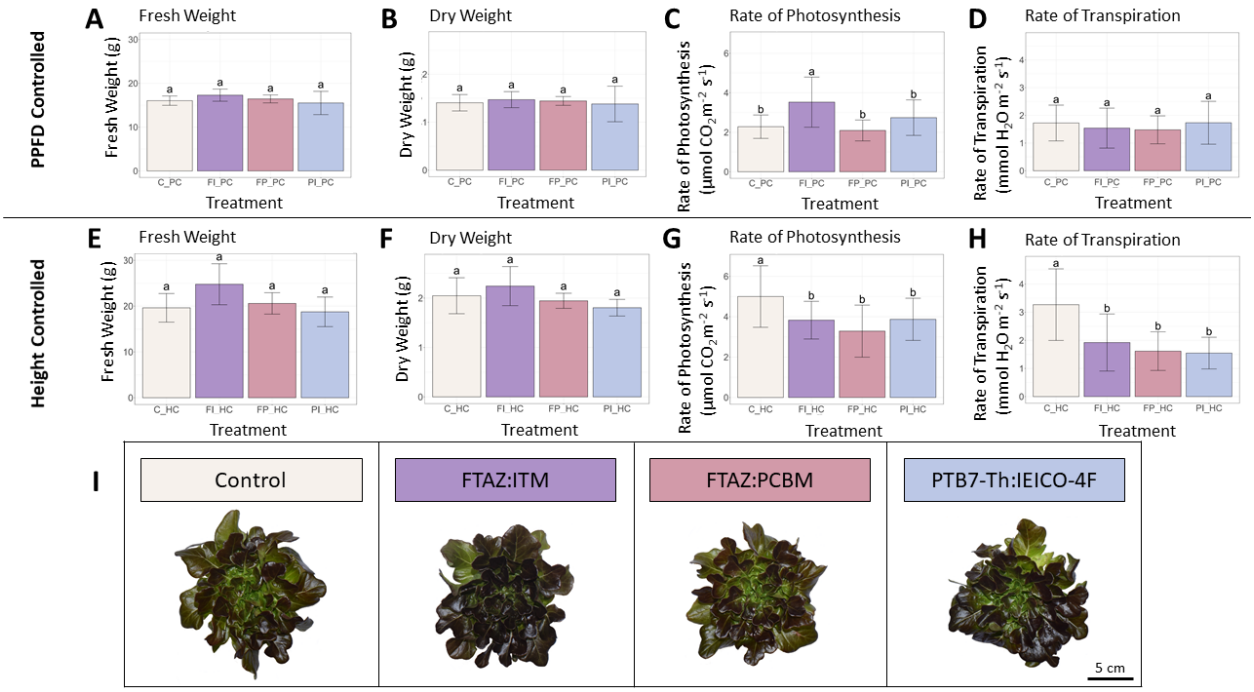

Figure 3. Lettuce biomass accumulation and carbon assimilation under OSC filters at harvest
a) Fresh weight of lettuce grown under OSC filters and clear glass control (C_PC) in the PC experiment. b) Dry weight of lettuce grown in each treatment in the PC experiment. c) Rate of photosynthesis (µmol CO_2 m^{-2} s^{-1}) measured under each light condition in the PC experiment. d) Transpiration rate (mmol H_2O m^{-2} s^{-1}) measured under each light condition in the PC experiment. e-h) Fresh weight, dry weight, photosynthetic and transpiration rates in the HC experiment (Ravishankar, et al., 2021). i) Representative photos of plants from each treatment in the PC experiment. Error bars represent the standard deviation. Statistical significance was assessed by ANOVA and Tukey test ($p<0.05$). For each plot, the differences between the means of treatments marked with the same letter are not statistically significant.

Photosynthesis was altered by filter spectra

Despite the fairly uniform growth, the filter spectra did affect the physiology of the lettuce. In the FI_PC treatment, the rate of photosynthesis was significantly higher than all other treatments in the PC experiment, and intercellular CO_2 was significantly lower (Fig. 3c, S1d). Unlike the HC experiment, where variation in photosynthesis was attributed to differences in light intensity (Ravishankar, et al., 2021) (Fig. 3g, h; S1g, h), these differences must be due to the spectrum of the FI filter. While filter degradation did result in some variation in light intensity by the end of the PC experiment (see Table 1; Fig. S3), the trends reported here remained after normalization to PPFD recorded at the time of measurement, although they were not always statistically significant (Fig. S4). The FI_PC treatment had more blue and red light relative to green light than the control. Red and blue light are used more efficiently than green light during photosynthesis due to the peak absorbance wavelengths of chlorophyll a and b (Eichhorn Bilodeau, et al., 2019) (Fig. 1d). This improved efficiency seems to have resulted in the higher rate of photosynthesis under the FI filter.

In contrast, the FP_PC treatment did not have a photosynthetic rate higher than control despite it also receiving more blue and red light relative to green (Fig. 3c). We attributed this difference to FP_PC's higher R/B ratio relative to FI_PC (4.5 and 2.7, respectively). Higher R/B

ratios have been shown to reduce stomatal conductance and decrease carbon assimilation in lettuce (Wang et al., 2016). Stomatal conductance was correspondingly lower than control in the FP_PC treatment, although the difference was not significant (Fig. S1c). Transpiration rate in the PC experiment was generally consistent across all treatments (Fig. 3d). This contrasts with the variation seen in the HC experiment (Fig. 3h), where transpiration rate was significantly different between each filter treatment and the control. This suggests that transpiration rate was predominantly controlled by light intensity and not the spectra produced by the three OSC filters studied here. Furthermore, when the transpiration rates from the HC experiment were normalized to PPFD recorded at the time of measurement, the differences between filter treatment and control were no longer significant (Fig. S4). As with biomass, the amount of light was more important than the spectrum in determining certain photosynthetic parameters such as transpiration rate. However, the quality of the light did appear to have a direct effect on the rate of photosynthesis, independent of light intensity.

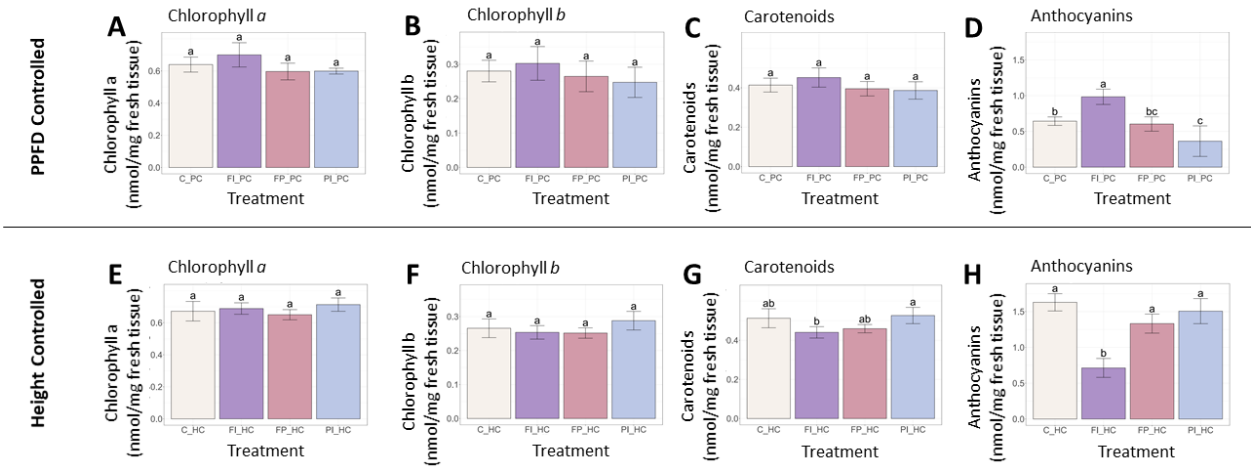

Figure 4. Secondary metabolites in lettuce leaf tissue under OSC filters at harvest
a) Ratio of chlorophyll a to chlorophyll b in sampled leaf tissue in the PC experiment. b) Carotenoid concentration in sampled leaf tissue in the PC experiment. c) Anthocyanin concentration in sampled leaf tissue in the PC experiment. Furthermore, PI_PC had a significantly lower anthocyanin concentration relative to the control despite having a very similar amount of blue light, 47 µmol m^{-2} s^{-1} or 16% of TPFD relative to 52 µmol m^{-2} s^{-1} or 15% for FI_PC. When the PC experiment was replicated and normalized as described above (Fig S7), the anthocyanins in FI_PC remained significantly higher than all other treatments, although the PI_PC treatment was no longer significantly lower than control. d-f) Chlorophyll a/b, carotenoids and anthocyanins in the HC experiment. Error bars represent the standard deviation. Statistical significance was assessed by ANOVA and Tukey test ($p<0.05$). For each plot, the differences between the means of treatments marked with the same letter are not statistically significant.

Anthocyanin content was significantly higher under the FI filter

Certain secondary metabolites with photosynthetic relevance were extracted from leaf tissue to look for acclimation to the altered light environment under the OSC filters. Chlorophyll, for example, has been shown to increase in overall concentration in response to a lower R/B ratio (Wang et al 2016). Surprisingly, there were no significant differences in chlorophyll *a* or *b* in neither the PC nor HC experiments (Fig. 4a, b, e, f), nor were there significant differences in the ratio of chlorophyll *a* to *b* in either experiment (Fig. S14), which has been shown to correlate with light intensity (Evans, 1988). In contrast, the carotenoids and anthocyanins that protect the

plant by absorbing excess light varied between treatments. In the HC experiment, both carotenoids and anthocyanins were significantly lower in the FI_HC treatment relative to the control (Fig. 4g, h). This corresponds with the reduced light intensity (both PPFD and TPFD) seen in FI_HC. Additionally, when this experiment was replicated and the results were normalized relative to the control treatment of each temporal replicate, C_HC, the high light control, had significantly more anthocyanins than all other treatments (Fig. S7).

The FI_PC treatment had significantly a higher anthocyanin content than all other PC treatments (Fig. 4d). Despite receiving approximately the same amount of light, the plants in this treatment accumulated more anthocyanins than those under the other filters or the white light control. While anthocyanin content in lettuce has been shown to increase with exposure to UV light (Park, et al., 2007), increased blue light (Stutte, 2009) and increased light intensity (Zhang, et al., 2018), the differences in blue light and total light intensity between the FI_PC treatment and the other treatments were small (~15 μmol m^{-2} s^{-1} blue and ~70 μmol m^{-2} s^{-1} TPFD), and all treatments lacked UV light. This suggests that aspects of the FI transmission spectrum enhanced anthocyanin content beyond what could be expected from the amount of blue light it transmits.

Gene expression networks identified genomic responses

The consensus network identified 35 modules ranging in size from 39 to 3,656 genes, represented in the cluster dendrogram (Fig. S8). Genes within a given module are considered to have highly similar expression profiles. Each module is described by a single value called the module eigengene that represents the expression profile of the entire module. These module eigengenes were used to assess relationships between gene expression profiles and quantitative measures of light quality, such as TPFD, R/B ratio, red to far-red (R/FR) ratio as well as physiological parameters (e.g. anthocyanin concentration). We identified clusters of genes that responded similarly to these parameters by comparing the sign of the correlation between the module eigengene and each quantitative measurement between the PC and HC experiments. Module 2 (2,397 genes) showed a strong positive correlation with TPFD in both PC and HC experiments (r=0.9, p=1e-07 and r=0.7, p=0.002, respectively, Fig. 5, S9), indicating that genes in this module are strongly influenced by small increases in light intensity. Module 12 (3,656 genes) also showed a strong correlation with TPFD but in the opposite direction (r=-0.8, p=3e-05 and r=-0.7, p=0.002). This suggests an inverse relationship between genes in Module 2 and Module 12, where higher values of TPFD are associated with higher expression of genes in Module 2 but lower expression in Module 12.

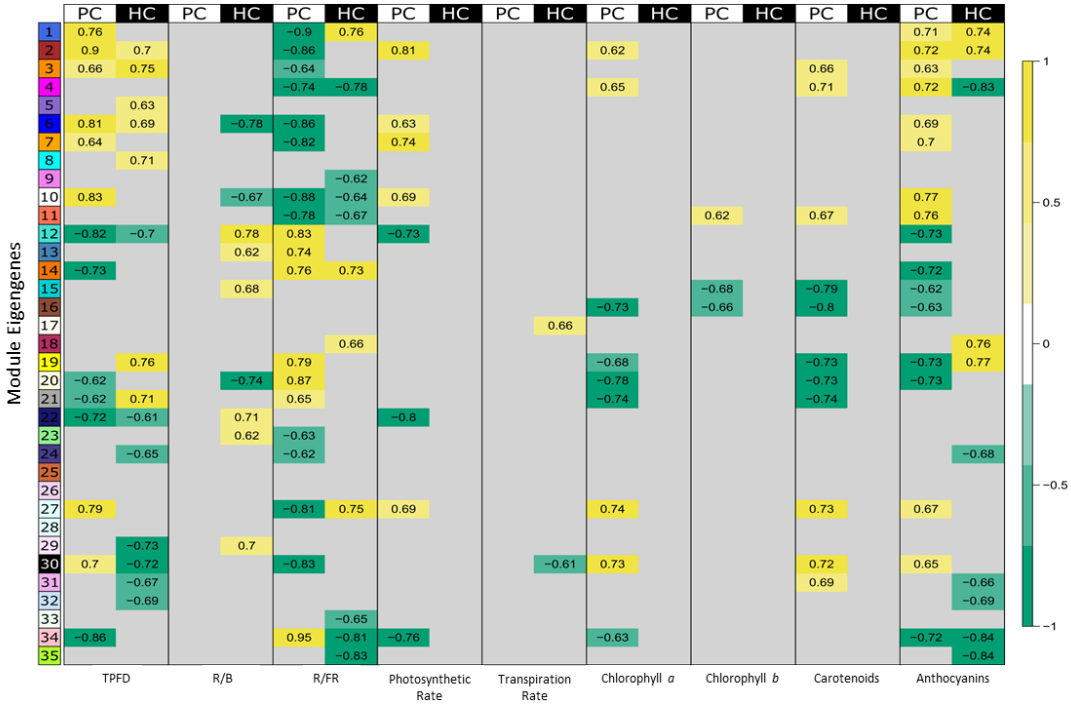

Figure 5. Module-trait relationships with selected light and physiological traits
Table of correlations between measured light and physiological parameters and the 35 modules of genes identified in the network analysis. Strong positive correlations are dark yellow while strong negative correlations are dark green. Values given are the correlation coefficient (*r*) for each relationship. Parameters such as TPFD tended to have correlations in the same direction for both PC and HC experiments. Others had significant correlations when only spectrum varied in the PC experiment or in response to both spectral and light intensity changes in the HC experiment. Modules showing weak or no significant correlation with a trait were filtered by applying a p-value threshold (p<1e-05). See Figure S9 for the unfiltered module-trait correlation table.

The same two modules also had opposite correlations with the R/FR ratio in the PC experiment but not the HC experiment (Fig. 5, Fig. S9). When light intensity was consistent in the PC experiment, Module 2 was negatively correlated with the R/FR ratio, meaning that these genes tended to have higher expression when lettuce was grown under a lower R/FR ratio (*r*=-0.9, p=3e-06). However, when light intensity varied in addition to the spectrum, the correlation between the Module 2 eigengene and the R/FR ratio was not significant (p=0.05). A similar pattern was seen in Module 12 where there was a positive correlation with the R/FR ratio in the PC experiment (*r*=0.8, p=1e-05) but no significant correlation in the HC experiment (p=0.8). The lack of correlation with the R/FR ratio for both modules in the HC experiment is further evidence that these genes are highly sensitive to light intensity. While these genes are responsive to the R/FR ratio as seen in the PC experiment, their expression correlates more strongly with TPFD (i.e. light intensity) when both intensity and spectrum are varied in the HC experiment. Other interesting trends were seen with other traits, particularly the R/B ratio that had significant correlations with several modules in the HC experiment and none in the PC experiment.

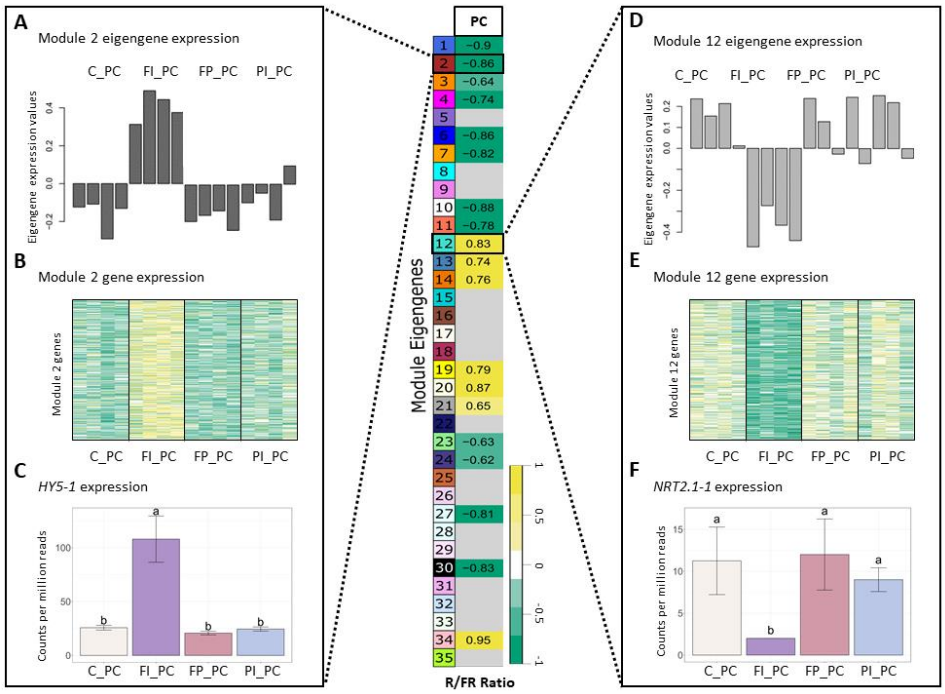

Figure 6. Gene expression of Modules 2 and 12 and correlation with R/FR ratio
Module-trait relationship between the R/FR (red/far-red) ratio and Modules 2 and 12 with gene expression characteristic of each module. a) Normalized expression of the Module 2 eigengene expression for each of the PC treatments by sample. b) Heatmap of gene expression for all genes in Module 2, where dark yellow indicates a strong increase in expression and dark green indicates a strong decrease in expression. c) Normalized gene expression of a Module 2 hub gene, *elongated hypocotyl 5* (*HY5-1*). As there are two genes identified in the lettuce genome as *HY5* and both are strongly correlated with Module 2 in the PC experiment (kME= 0.9 and 0.9, p= 2e-07 and 1e-6, Appendix S3), one was chosen to be discussed in detail and is designated *HY5-1* (LOC111908039). d-f) Eigengene expression, gene expression and hub gene expression (*high-affinity nitrate transporter 2.1*, *NRT2.1-1*) for Module 12. The treatment with the lowest R/FR ratio, FI_PC (FTAZ:IT-M filter in the PC experiment), had higher gene expression in Module 2, resulting in a negative correlation with the R/FR ratio. In contrast, Module 12 had a positive correlation with R/FR ratio due to the downregulation of expression in FI_PC, relative to the other treatments. These trends are exemplified in hub genes of each module: *HY5-1* in Module 2 and *NRT2.1-1*. Table values given are the correlation coefficient (*r*) for each relationship. Insignificant correlations were removed (p<1e-05). Error bars indicate the standard deviation. Letters indicate significance from ANOVA and Tukey test (p<0.05). See Figure S9 for full table.

We identified genes whose expression patterns were highly correlated with a particular module and its representative eigengene in Modules 2 and 12 to investigate the R/FR dependence. These genes are referred to as hub genes as they are considered to be highly connected to the other genes in that module and represent the key drivers of module-trait associations. One hub gene in Module 2 is *elongated hypocotyl 5* (*HY5)*, which encodes a light-responsive transcription factor important for photomorphogenesis (Abbas, et al., 2014). As expected of a hub gene, *HY5-1* expression closely matches the pattern of both Module 2 eigengene expression and the overall expression of all Module 2 genes (Fig. 6). Accordingly, *HY5* expression is also negatively correlated with R/FR, suggesting that *HY5* expression increases in response to lower R/FR ratios. Indeed, the treatment with the lowest R/FR ratio in the PC experiment, FI_PC (Appendix S4), also had the highest expression of *HY5-1*. Conversely, a *high affinity nitrate transporter 2.1* gene (*NRT2.1-1*, LOC111883156), a hub gene of Module 12 in the PC experiment (kME=0.9, p=2e-06), has an opposite expression pattern with the lowest

expression in FI_PC, compared to the other treatments. Surprisingly, HY5 has been identified as an enhancer of NRT2.1 and was expected to increase, not decrease, expression of its target, a gene important for nitrate uptake and nutrient acquisition (Chen, et al., 2016).

Gene expression related to anthocyanins was altered under FI filter

We conducted a differential gene expression analysis separately for the PC and HC experiments to quantify changes in the expression of individual genes between each filter treatment and its control (Table S1), as well as a DEG analysis that compared HC filter treatments to their respective PC treatments (Fig. S10, Table S3). The expression patterns seen in the photoreceptors reflect the light environment of the plants in both experiments (Table 1, Fig. S11). When both light intensity and spectrum varied, FI_HC, FP_HC and PI_HC all had many differentially expressed genes (DEGs) relative to the C_HC control (395, 1,700 and 144, respectively, $p<1e-05$). This variation reflects the large differences in TPFD and spectra in the HC experiment. On the other hand, fewer differences were observed for all filter treatments relative to the control except FI_PC when TPFD was controlled in the PC experiment. There were 1,143 DEGs identified in the FI_PC/C_PC comparison but only 15 DEGs in FP_PC/C_PC and 12 DEGs in PI_PC/C_PC ($p<1e-05$). While filter degradation did result in changes in TPFD by the end of the PC experiment, this small variation in light intensity alone cannot account for the large differences between the FI_PC treatment and the other treatments. As reported earlier, gene expression of several large modules of genes correlated with the R/FR ratio as well as TPFD in this experiment. This suggests that the R/FR ratio and possibly other spectral characteristics unique to the FI filter resulted in differential gene expression. In particular, *HY5-1* gene expression was increased by a $\log_2$ fold change of 2.2 in FI_PC, which is consistent with a previous study that found that *HY5* expression increased with lower R/FR ratios (van Gelderen, et al., 2021). Because HY5 is a transcription factor that controls expression of many downstream genes, it is not surprising that many of these genes were also differentially expressed in the FI_PC treatment. Among these were several anthocyanin modification enzymes that were upregulated relative to the PC control (Table S1). The increase in expression of anthocyanin modification genes is supported by the increase in anthocyanin concentration seen in Figure 5, where the FI_PC treatment had a significantly higher concentration than all other treatments. Other genes known to be directly or indirectly regulated by HY5 were also upregulated, including several related to nitrate uptake, defense against predation and the circadian clock (Table S1).

Discussion

Our experiments were designed to account for both the quantitative and qualitative aspects of OSC-filtered light on lettuce as a representative crop. Despite the morphological similarities between treatments, the physiology of the plants was altered by the differences in light quality under the OSC filters on a molecular and transcriptomic level.

Transcriptome analysis identified physiological and metabolic changes

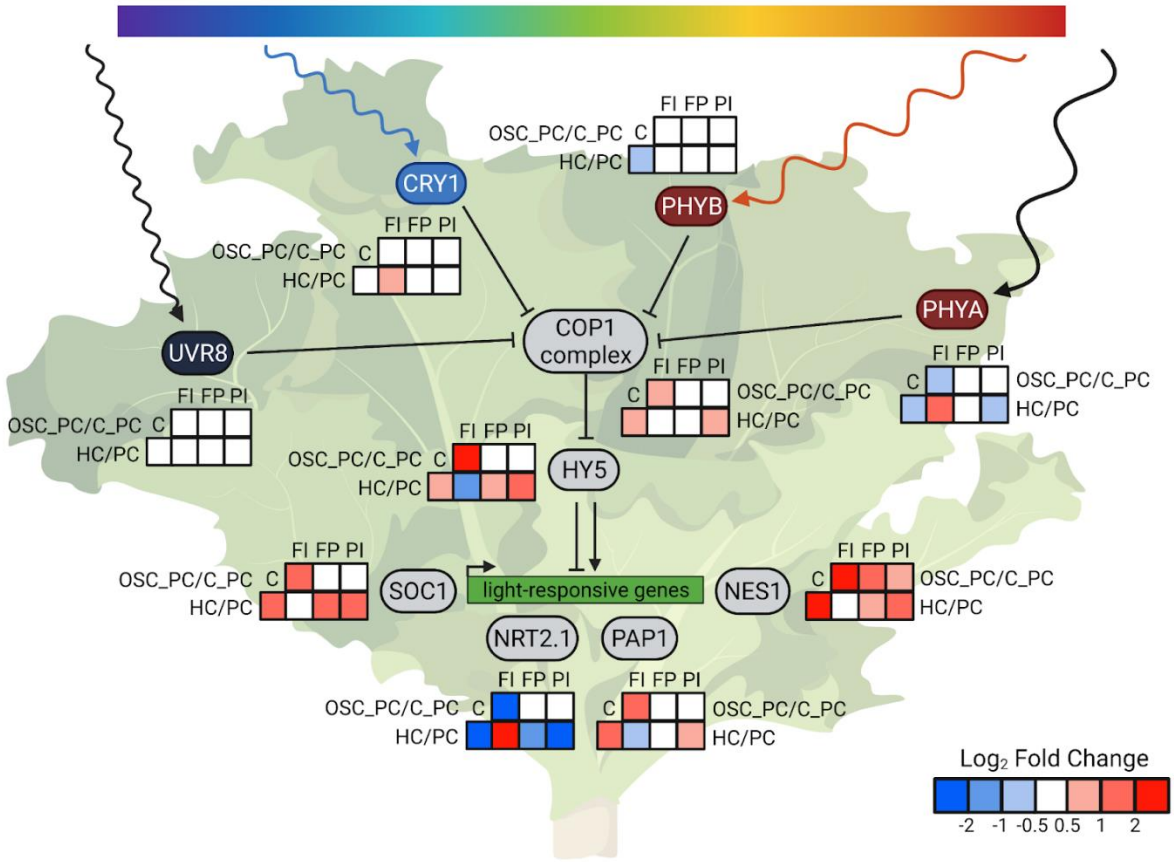

Figure 7. HY5 integrates light signals and regulates downstream genes
Condensed photoreceptor signaling pathway with downstream genes of interest. The photoreceptors indirectly upregulate expression of *HY5* through inhibition of the constitutive photomorphogenic 1 (COP1) complex formation. Elongated hypocotyl 5 (HY5-1) is a transcription factor that is a known or hypothesized regulator of many light-responsive genes, including *suppressor of overexpression of CO 1* (*SOC1*), *high affinity nitrate transporter 2.1* (*NRT2.1-1*), *production of anthocyanin pigment1/MYB75* (*PAP1*) and *(3S,6E)-nerolidol synthase 1* (*NES1-1*). Beginning with the photoreceptors that sense light, expression of many genes was altered by changes in either light intensity or light quality, or both (Fig. S11). These photoreceptors, along with the cryptochromes, inhibit the formation of the complex that COP1 ubiquitin ligase forms with suppressor of phyA 105-1 (SPA1), which prevents the degradation of transcription factors such as HY5 and leads to photomorphogenesis (Abbas, et al., 2014). Our analysis revealed that *COP1* itself was differentially expressed in response to both light quality changes (FI_PC/C_PC) and intensity changes (C_HC/C_PC and PI_HC/PI_PC). The changes in *COP1* expression are in the opposite direction of many of the trends observed in *phyA1* expression. This may indicate that the expression of *COP1*, in addition to activity of its protein, is regulated by light. Relative transcript abundance is represented by $\log_2$ fold changes between specified treatments. Created with BioRender.com.

HY5 was differentially expressed in response to altered spectrum (FI_PC/C_PC) and altered light quantity (HC/PC for each spectrum) (Fig. 7). *HY5* expression is regulated by the COP1 complex (Abbas, et al., 2014). The expression of several light-responsive genes was also altered in response to changes in spectrum and the overall amount of light. One of these genes is *suppressor of overexpression of CO 1* (*SOC1*), a transcription factor that regulates flowering and has been identified as a putative target of HY5 (Lee, et al., 2007; Lee and Lee, 2010). That this gene was upregulated under the FI filter relative to the control with similar light intensity suggests that the spectrum produced by an OSC greenhouse utilizing FI as its active layer may trigger an earlier flowering time in plants. The regulation of flowering is an important aspect of

crop development that can impact harvest. In particular, the prevention of early flowering in lettuce can improve harvests by extending the growing period before the lettuce begins to bolt, altering its metabolite and flavor profile (Hao, et al., 2018). Although this would be undesirable in lettuce, this effect was not seen in the other OSC filters tested, which yielded similar biomass.

Although the FI filter seems to negatively impact bolting, it may yield improved defense from insect predation. *(3S,6E)-nerolidol synthase 1* (*NES1-1*) gene expression increased in response to both light intensity and altered spectrum (Fig. 7). While it has not been demonstrated that *NES1* is directly regulated by HY5, it is a known regulator in the terpenoid synthase pathway of which *NES1* is a member (Michael, et al., 2020). *NES1* encodes an enzyme that produces nerolidol, a volatile compound released by the plant in response to wounding by herbivorous insects. This molecule has been shown to attract predator insects in tea plants, protecting the plants from further damage by reducing the number of pests (Naskar, et al., 2021). A primed defense system may further reduce the use of pesticides in OSC greenhouses. Crops less suited to greenhouses (e.g. orchards) that can be grown under elevated OSC panels (Toledo and Scognamiglio, 2021) would benefit even more from increased predation defense.

Impacts from OSC spectra on nutrient content

Crops rich in anthocyanins are more nutritious and have a positive effect on human health when included in the diet (Cerletti, et al., 2017). Anthocyanin content in red cultivars of lettuce has been shown to increase in response to increased light intensity (Zhang, et al., 2018) and altered spectrum (Sng, et al., 2021; Stutte, 2009). Production of anthocyanin pigment 1/MYB75 (PAP1) is a transcription factor that regulates anthocyanin accumulation and whose gene expression is directly regulated by HY5 (Gangappa and Botto, 2016). Accordingly, *PAP1* expression mirrored the trends seen in *HY5* (Fig. 7). This provides a genomic and molecular basis for the increase in anthocyanin content seen in the FI_PC treatment relative to the other PC treatments (Fig. 4).

While nitrate is required for growth and must be supplied in fertilizer, high nitrate content in lettuce leaves is an important consumer concern with human health effects (Li, et al., 2021). Several nitrogen transporter genes were differentially expressed in the FI_PC treatment relative to control, including *NRT2.1-1* (Fig. 7, Table S1). A recent study has demonstrated that HY5 can act as a negative regulator of *NRT2.1* under certain conditions (van Gelderen, et al., 2021). It should also be noted that much of the research on NRT2.1 is focused on nitrate uptake from the soil and is primarily analyzing expression in root, not leaf, tissue. The downregulation of nitrate transporters in leaf tissue may indicate that nitrate is selectively reduced in the roots instead of the leaves and accumulates less in the leaves. Additionally, the decrease in *nitrate reductase* (*NR*) expression could indicate lessened demand for the conversion of nitrate (NO^-_3) to nitrite (NO^-_2) in the leaves (Table S1, Fig. S12). As nitrate levels in lettuce have been shown to vary in response to different light intensities (Fu, et al., 2017), these changes may correlate with desirable low nitrate levels in leaf tissue and improved nutrition in addition to changes in nitrogen use efficiency and fertilizer requirements.

Conclusions

The experiments presented here offer molecular insight into plant growth and development under OSC filters. We found no negative impacts on the accumulation of biomass or on the quantified secondary metabolites when light intensity was controlled. The differential gene expression,

especially the upregulation of key regulator genes under the FI filter, is worthy of further study to discover how these changes translate to important aspects of crop production. In particular, the gene expression changes related to the initiation of flowering pointed to economic impacts for crops like lettuce, where early flowering can damage harvests by introducing a bitter taste, and tomato, where early flowering and fruit development can increase yields. The advantage of a transcriptome analysis in the study of OSC-grown plants is that these key modifications can be identified without the need to directly measure each aspect of plant growth and development. The reduced climate impact of OSC-integrated greenhouses comes with the potential to not only produce many crop species at a marketable price but to enable growers to fine-tune plant characteristics by selecting from the wide range of OSC transmission spectra.

Acknowledgements

We would like to thank Jennifer Swift for technical assistance and the NSF INFEWS grant (award 1639429) for its support.

References

Abbas N, Maurya JP, Senapati D, Gangappa SN, Chattopadhyay S (2014) Arabidopsis CAM7 and HY5 Physically Interact and Directly Bind to the HY5 Promoter to Regulate Its Expression and Thereby Promote Photomorphogenesis. The Plant cell **26:** 1036-1052

Barbosa GL, Gadelha FDA, Kublik N, Proctor A, Reichelm L, Weissinger E, Wohlleb GM, Halden RU (2015) Comparison of land, water, and energy requirements of lettuce grown using hydroponic vs. conventional agricultural methods. International journal of environmental research and public health **12:** 6879-6891

Cerletti C, De Curtis A, Bracone F, Digesù C, Morganti AG, Iacoviello L, de Gaetano G, Donati MB (2017) Dietary anthocyanins and health: data from FLORA and ATHENA EU projects. British journal of clinical pharmacology **83:** 103-106

Chen X, Yao Q, Gao X, Jiang C, Harberd N, Fu X (2016) Shoot-to-Root Mobile Transcription Factor HY5 Coordinates Plant Carbon and Nitrogen Acquisition. Current biology **26:** 640-646

De Villiers DS, Wien HC, Reid JE, Albright LD (2009) Energy use and yields in tomato production: Field, high tunnel and greenhouse compared for the northern tier of the USA (upstate New York). 373-380

Edgar R, Domrachev M, Lash AE (2002) Gene Expression Omnibus: NCBI gene expression and hybridization array data repository. Nucleic acids research **30:** 207-210

Eichhorn Bilodeau S, Wu B, Rufyikiri A, MacPherson S, Lefsrud M (2019) An Update on Plant Photobiology and Implications for Cannabis Production. Frontiers in plant science **10:** 296

Emmott CJM, Röhr JA, Campoy-Quiles M, Kirchartz T, Urbina A, Ekins-Daukes NJ, Nelson J (2015) Organic photovoltaic greenhouses: a unique application for semi-transparent PV? Energy & environmental science **8:** 1317-1328

Evans JR (1988) Acclimation by the Thylakoid Membranes to Growth Irradiance and the Partitioning of Nitrogen Between Soluble and Thylakoid Proteins. Functional plant biology : FPB **15:** 93-106

Galvao VC, Fankhauser C (2015) Sensing the light environment in plants: photoreceptors and early signaling steps. Curr Opin Neurobiol **34:** 46-53
Gangappa S, Botto J (2016) The Multifaceted Roles of HY5 in Plant Growth and Development. Molecular plant **9:** 1353-1365
Guo H, Yang H, Mockler TC, Lin C (1998) Regulation of flowering time by Arabidopsis photoreceptors. Science (American Association for the Advancement of Science) **279:** 1360-1363
Hahm J, Kim K, Qiu Y, Chen M (2020) Increasing ambient temperature progressively disassemble Arabidopsis phytochrome B from individual photobodies with distinct thermostabilities. Nature Communications **11:**
Hao J, Zhang L, Li P, Sun Y, Li J, Qin X, Wang L, Qi Z, Xiao S, Han Y, Liu C, Fan S (2018) Quantitative Proteomics Analysis of Lettuce (Lactuca sativa L.) Reveals Molecular Basis-Associated Auxin and Photosynthesis with Bolting Induced by High Temperature. International journal of molecular sciences **19:** 2967
Hassanien RHE, Li M, Lin WD (2016) Advanced applications of solar energy in agricultural greenhouses. Renewable and Sustainable Energy Reviews **54:** 989-1001
Hollingsworth JA, Ravishankar E, O'Connor B, Johnson JX, DeCarolis JF (2020a) Environmental and economic impacts of solar-powered integrated greenhouses. Journal of Industrial Ecology **24:** 234-247
Hollingsworth JA, Ravishankar E, O'Connor B, Johnson JX, DeCarolis JF (2020b) Environmental and economic impacts of solar-powered integrated greenhouses. Journal of industrial ecology **24:** 234-247
Jain M, Sharma P, Tyagi SB, Tyagi AK, Khurana JP (2007) Light regulation and differential tissue-specific expression of phototropin homologues from rice (Oryza sativa ssp. indica). Plant science (Limerick) **172:** 164-171
Khan MRG, Ai X, Zhang J (2014) Genetic regulation of flowering time in annual and perennial plants. Wiley interdisciplinary reviews. RNA **5:** 347-359
Kim D, Langmead B, Salzberg SL (2015) HISAT: a fast spliced aligner with low memory requirements. Nature methods **12:** 357-360
Kim H, Lin M, Mitchell CA (2019) Light spectral and thermal properties govern biomass allocation in tomato through morphological and physiological changes. Environmental and experimental botany **157:** 228-240
Kohler AE, Lopez RG (2021) Duration of light-emitting diode (LED) supplemental lighting providing far-red radiation during seedling production influences subsequent time to flower of long-day annuals. Scientia horticulturae **281:** 109956
Langfelder P, Horvath S (2012) Fast R Functions for Robust Correlations and Hierarchical Clustering. Journal of statistical software **46:**
Langfelder P, Horvath S (2008) WGCNA: an R package for weighted correlation network analysis. BMC bioinformatics **9:** 559
Lee J, He K, Stolc V, Lee H, Figueroa P, Gao Y, Tongprasit W, Zhao H, Lee I, Deng XW (2007) Analysis of Transcription Factor HY5 Genomic Binding Sites Revealed Its Hierarchical Role in Light Regulation of Development. THE PLANT CELL **19:** 731-749
Lee J, Lee I (2010) Regulation and function of SOC1, a flowering pathway integrator. Journal of experimental botany **61:** 2247-2254
Liao Y, Smyth GK, Shi W (2014) Featurecounts: an efficient general purpose program for assigning sequence reads to genomic features. Bioinformatics (Oxford, England) **30:** 923-930

Luo Q, Li Y, Gu H, Zhao L, Gu X, Li W (2013) The promoter of soybean photoreceptor GmPLP1 gene enhances gene expression under plant growth regulator and light stresses. Plant Cell Tiss Organ Cult **114:** 109-119

McCarthy DJ, Chen Y, Smyth GK (2012) Differential expression analysis of multifactor RNA-Seq experiments with respect to biological variation. Nucleic acids research **40:** 4288-4297

Naskar S, Roy C, Ghosh S, Mukhopadhyay A, Hazarika LK, Chaudhuri RK, Roy S, Chakraborti D (2021) Elicitation of biomolecules as host defense arsenals during insect attacks on tea plants. Applied microbiology and biotechnology **105:** 7187

Park J, Choung M, Kim J, Hahn B, Kim J, Bae S, Roh K, Kim Y, Cheon C, Sung M, Cho K (2007) Genes up-regulated during red coloration in UV-B irradiated lettuce leaves. Plant Cell Rep **26:** 507-516

Pattison PM, Tsao JY, Brainard GC, Bugbee B (2018a) LEDs for photons, physiology and food. Nature **563:** 493-500

Pattison PM, Tsao JY, Brainard GC, Bugbee B (2018b) LEDs for photons, physiology and food. Nature (London) **563:** 493-500

Ravishankar E, Booth RE, Hollingsworth JA, Ade HW, Sederoff H, DeCarolis J, O'Connor BT (2022) Organic solar powered greenhouse performance optimization and global economic opportunity. *Energy & Environmental Science* DOI: 10.1039/D1EE03474J

Ravishankar E, Booth RE, Saravitz C, Sederoff H, Ade HW, O'Connor BT (2020) Achieving net zero energy greenhouses by integrating semitransparent organic solar cells. Joule **4:** 490-506

Ravishankar E, Charles M, Xiong Y, Henry R, Swift J, Rech J, Calero J, Cho S, Booth RE, Kim T, Balzer AH, Qin Y, Hoi Yi Ho C, So F, Stingelin N, Amassian A, Saravitz C, You W, Ade H, Sederoff H, O'Connor BT (2021) Balancing crop production and energy harvesting in organic solar-powered greenhouses. Cell Reports Physical Science **2:** 100381

Reyes-Chin-Wo S, Wang Z, Yang X, Kozik A, Arikit S, Song C, Xia L, Froenicke L, Lavelle DO, Truco M, Xia R, Zhu S, Xu C, Xu H, Xu X, Cox K, Korf I, Meyers BC, Michelmore RW (2017) Genome assembly with in vitro proximity ligation data and whole-genome triplication in lettuce. Nature communications **8:** 14953

Robinson MD, McCarthy DJ, Smyth GK (2010) edgeR: a Bioconductor package for differential expression analysis of digital gene expression data. Bioinformatics **26:** 139-140

Sharrock RA, Quail PH (1989) Novel phytochrome sequences in Arabidopsis thaliana: structure, evolution, and differential expression of a plant regulatory photoreceptor family. Genes & development **3:** 1745-1757

Sims DA, Gamon JA (2002) Relationships between leaf pigment content and spectral reflectance across a wide range of species, leaf structures and developmental stages. Remote sensing of environment **81:** 337-354

Stutte GW (2009) Light-emitting Diodes for Manipulating the Phytochrome Apparatus. HortScience **44:** 231-234

Susan A. Dudley, Johanna Schmitt, Associate Editor: Ruth G. Shaw, Massimo Pigliucci (1999) Manipulative Approaches to Testing Adaptive Plasticity: Phytochrome-Mediated Shade-Avoidance Responses in Plants. The American naturalist **154:** S43-S54

Suzuki H, Nakayama T, Yonekura-Sakakibara K, Fukui Y, Nakamura N, Yamaguchi M, Tanaka Y, Kusumi T, Nishino T (2002) cDNA Cloning, Heterologous Expressions, and Functional Characterization of Malonyl-Coenzyme A:Anthocyanidin 3-O-Glucoside-6"-O-Malonyltransferase from Dahlia Flowers. PLANT PHYSIOLOGY **130:** 2142-2151

Tanaka Y, Sasaki N, Ohmiya A (2008) Biosynthesis of plant pigments: anthocyanins, betalains and carotenoids. The Plant journal : for cell and molecular biology **54:** 733-749
Tian Y, Wang H, Sun P, Fan Y, Qiao M, Zhang L, Zhang Z (2019) Response of leaf color and the expression of photoreceptor genes of Camellia sinensis cv. Huangjinya to different light quality conditions. Scientia horticulturae **251:** 225-232
Toledo C, Scognamiglio A (2021) Agrivoltaic Systems Design and Assessment: A Critical Review, and a Descriptive Model towards a Sustainable Landscape Vision (Three-Dimensional Agrivoltaic Patterns). Sustainability (Basel, Switzerland) **13:** 6871
USDA, National Agricultural Statistics Service (2020) Vegetables 2019 Summary (February 2020). United States Department of Agriculture
van Gelderen K, Kang C, Li P, Pierik R (2021) Regulation of Lateral Root Development by Shoot-Sensed Far-Red Light via HY5 Is Nitrate-Dependent and Involves the NRT2.1 Nitrate Transporter. Frontiers in plant science **12:** 660870
Waller R, Kacira M, Magadley E, Teitel M, Yehia I (2021) Semi-Transparent Organic Photovoltaics Applied as Greenhouse Shade for Spring and Summer Tomato Production in Arid Climate. Agronomy (Basel) **11:** 1152
Xiao S, Zhang Q, You W (2017) Molecular Engineering of Conjugated Polymers for Solar Cells: An Updated Report. Advanced materials (Weinheim) **29:** 1601391-n/a
Zhang Y, Xu S, Cheng Y, Peng Z, Han J (2018) Transcriptome profiling of anthocyanin-related genes reveals effects of light intensity on anthocyanin biosynthesis in red leaf lettuce. PeerJ (San Francisco, CA) **6:** e4607
Zhen S, Bugbee B (2020) Far-red photons have equivalent efficiency to traditional photosynthetic photons: Implications for redefining photosynthetically active radiation. Plant, cell and environment **43:** 1259-1272
Zisis C, Pechlivani EM, Tsimikli S, Mekeridis E, Laskarakis A, Logothetidis S (2019) Organic Photovoltaics on Greenhouse Rooftops: Effects on Plant Growth. Materials today : proceedings **19:** 65-72